

Co-transfection with *BMP2* and *FGF2* via chitosan nanoparticles potentiates osteogenesis in human adipose-derived stromal cells *in vitro*

Journal of International Medical Research

49(3) 1–14

© The Author(s) 2021

Article reuse guidelines:

sagepub.com/journals-permissions

DOI: 10.1177/0300060521997679

journals.sagepub.com/home/imr



Ying Hu^{1,*} , Qing-Wei Zhao^{2,*},
Zheng-Cai Wang¹, Qing-Qing Fang¹, He Zhu²,
Dong-Sheng Hong², Xing-Guang Liang²,
Dong Lou¹ and Wei-Qiang Tan¹ 

Abstract

Objective: To investigate if co-transfection of human bone morphogenetic protein 2 (*BMP-2*, *BMP2*) and human fibroblast growth factor 2 (*FGF2*, *FGF2*) via chitosan nanoparticles promotes osteogenesis in human adipose tissue-derived stem cells (ADSCs) *in vitro*.

Materials and Methods: Recombinant *BMP2* and/or *FGF2* expression vectors were constructed and packaged into chitosan nanoparticles. The chitosan nanoparticles were characterized by atomic force microscopy. Gene and protein expression levels of *BMP-2* and *FGF2* in ADSCs *in vitro* were evaluated by real-time polymerase chain reaction (PCR), western blot, and enzyme-linked immunosorbent assay. Osteocalcin (OCN) and bone sialoprotein (BSP) gene expression were also evaluated by real-time PCR to assess osteogenesis.

Results: The prepared chitosan nanoparticles were spherical with a relatively homogenous size distribution. The *BMP2* and *FGF2* vectors were successfully transfected into ADSCs. *BMP-2* and *FGF2* mRNA and protein levels were significantly up-regulated in the co-transfection group compared with the control group. OCN and BSP mRNA levels were also significantly increased in the co-transfection group compared with cells transfected with *BMP2* or *FGF2* alone, suggesting that co-transfection significantly enhanced osteogenesis.

*These authors contributed equally to this work.

¹Department of Plastic Surgery, Sir Run Run Shaw Hospital, Zhejiang University School of Medicine, Hangzhou, PR China

²Department of Clinical Pharmacy, The First Affiliated Hospital, Zhejiang University School of Medicine, Hangzhou, PR China

Corresponding author:

Wei-Qiang Tan, Department of Plastic Surgery, Sir Run Run Shaw Hospital, Zhejiang University School of Medicine, 3 East Qingchun Road, Hangzhou, 310016, Zhejiang Province, PR China.
Email: tanweixxx@zju.edu.cn



Conclusions: Co-transfection of human ADSCs with *BMP2/FGF2* via chitosan nanoparticles efficiently promotes the osteogenic properties of ADSCs *in vitro*.

Keywords

Chitosan nanoparticle, bone morphogenetic protein-2, basic fibroblast growth factor, adipose tissue-derived stem cell, osteogenesis, osteocalcin, bone sialoprotein

Date received: 31 January 2021; accepted: 4 February 2021

Introduction

Trauma, infection, and cancer can cause bony defects, which can in turn lead to dysfunction and deformity, with an immense impact on patient quality of life.^{1,2} Traditional therapy for bone defects is generally ineffective; however, gene therapy, which aims to maintain local bone growth factors at a therapeutic concentration, is a promising method for boosting the healing of bone defects.³ Other advantages of gene therapy include the controlled release of target gene products, thereby maximizing local therapeutic effects and reducing systemic side effects.⁴ However, various techniques are available to deliver gene therapy, and there is still a lack of consensus regarding the optimal delivery system in the field of bone repair.

Re-vascularization is a crucial part of bone healing.⁵ Fibroblast growth factor 2 (FGF2, also known as basic FGF) is one of the most effective factors stimulating the migration and hyperplasia of capillary endothelial cells, the formation of capillary buds, and the secretion of plasminogen activators and collagenase.⁶ It also affects the degradation of the extracellular matrix in the wound,⁷ allowing capillaries to extend into the wound. Bone morphogenetic proteins (BMPs) are cytokines that have been proven to induce bone differentiation and are involved in osteogenesis. BMP-2 was the first BMP shown to induce differentiation towards cartilage and bone tissue

in vivo, and the local application of exogenous BMP-2 protein or bone marrow-derived mesenchymal stem cells (BMSCs) transfected with the BMP-2 gene (*BMP2*) was shown to aid the repair of bone defects.⁸

Franceschi et al.⁹ found that the osteogenic potential could be significantly improved by increasing expression levels of BMP-2, -4, and -7 via adenovirus-mediated transfection. Similarly, Gromolak et al.¹⁰ found that *in vitro* treatment of sheep BMSCs with FGF2 and BMP-2 led to increased expression of osteocalcin (OCN) and collagen type I and a series of osteogenic-related gene markers. We hypothesized that co-expression of FGF2 and BMP-2 via an effective gene delivery system would enhance osteogenesis. Chitosan nanoparticles are a non-viral gene-transfer technology that can transduce multiple genes.^{11,12} We therefore evaluated the *in vitro* osteogenic properties of human adipose tissue-derived stem cells (ADSCs) co-transfected with a *BMP2/FGF2* dual-gene system via chitosan nanoparticles.

Materials and Methods

Primary culture and identification of human ADSCs

Fat tissue was extracted from the omental fat of a healthy woman undergoing abdominal surgery. ADSCs were isolated by type I

collagenase digestion, as described by Peng et al.¹³ Briefly, fatty tissues were separated and washed in phosphate-buffered saline (PBS), and cells were dissociated for 30 minutes with 0.75% type I collagenase (1710001; Gibco, MA, USA) in Dulbecco's modified Eagle medium (DMEM; Gibco). After digestion, the digested cells were collected by centrifugation (4°C, 1000 × g for 10 minutes) and suspended in DMEM supplemented with 10% fetal bovine serum (FBS; Gibco), 100 U/mL penicillin, and 100 U/mL streptomycin (Sigma, MO, USA) in a humidified atmosphere containing 5% CO₂ at 37°C. The cells were grown to approximately 80% confluence, digested with 0.25% pancreatic enzyme/0.02% ethylenediaminetetraacetic acid (EDTA) solution, and the reaction was stopped with DMEM containing FBS before passage. The study protocol was approved by the Institutional Ethics Committee of Sir Run Run Shaw Hospital, Zhejiang University School of Medicine. The patient provided written consent for donating her fat tissues for research purposes.

To identify ADSCs, adherent P3 cells were harvested, washed, and suspended in fluorescence-activated cell sorting (FACS) buffer (Lonza, Basel, Switzerland). The cells were then incubated with human Fc block (564220, 1:10; BD Pharmingen, San Jose, CA, USA) for 15 minutes at 4°C followed by washing in FACS buffer twice, and incubated with anti-CD45-phycoerythrin, anti-CD31-allophycocyanin (APC), anti-CD34-fluorescein isothiocyanate (FITC), anti-CD44-APC, anti-CD29-FITC, and anti-CD105-APC for 45 minutes at 4°C, respectively. All the antibodies were purchased from BioLegend (San Diego, CA, USA). The cells were finally washed twice with FACS buffer and analyzed using a DxFLEX Flow Cytometer (Beckman Coulter Inc., Brea, CA, USA).

Construction of pEGFP-N2-hBMP-2/ pTagRFP-C-hFGF2 recombinant expression vectors

Full-length human *BMP2/FGF2* were cloned by Shanghai Biological Engineering Ltd. (Shanghai, China). The recovered gene fragments were inserted into pEGFP-N2/pTagRFP-C expression vectors (Genscript, Hangzhou, China) (Figure 1) at a

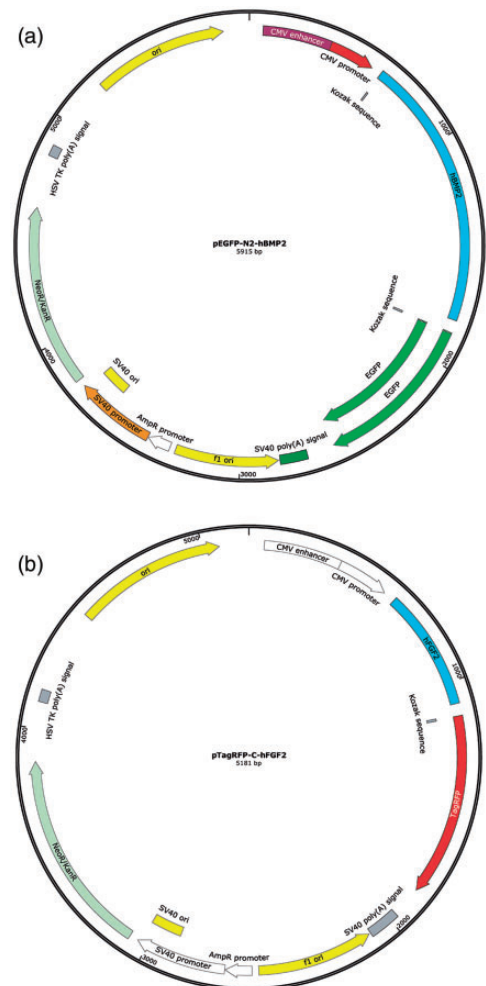


Figure 1. Diagram showing structures of recombinant expression vectors for over-expression of *BMP2* and *FGF2* *in vitro*. Schematic structures of (a) pEGFP-N2-hBMP-2 and (b) pTagRFP-C-hFGF2.

concentration ratio of 9:1 at 16°C for 8 hours using a Rapid DNA Ligation Kit (Thermo Fisher Scientific, MA, USA), according to the manufacturer's instructions) and then transformed into competent *Escherichia coli* JM 109 for amplification. pEGFP-N2-hBMP-2/pTagRFP-C-hFGF2 recombinant plasmids were extracted from *E. coli* JM109 using a Mini Plasmid Purification Kit (Macherey-Nagel GmbH & Co., Germany) according to the manufacturer's instructions. Recombinant plasmid vectors were verified by double restriction enzyme digestion: 1 µg of recombinant plasmid was digested by Bgl II and EcoR I at 37°C for 8 hours, and 5 µL of the digestion product was analyzed by agarose gel electrophoresis. Positive plasmids were also sequenced by TaKaRa Biotechnology Co., Ltd. (Dalian, China).

Construction of plasmid packaging chitosan nanoparticles and transfection

The chitosan nanoparticles were prepared largely according to the double emulsification solvent evaporation method.¹⁴ Briefly, two kinds of chitosan (448869; Sigma, C8320; Solarbio, China) were dissolved in 1% acetic acid (0.3 mg/mL, final concentration) and 0.01 M NaOH solution was added to adjust the pH to 5 to 6. The chitosan solution was sterilized using a vacuum filter (0.22 µm) (A solution). The constructed plasmids (containing *FGF2* and *BMP2*) were diluted in 100 µg/mL (B solution), and a 1:1 mixture of A and B solutions (containing either single or dual genes) was then used to obtain chitosan nanoparticles containing either the individual genes or both genes.

ADSCs were disseminated in 6-well plates at a concentration of 10⁶ cells per well. After 12 to 20 hours, 50 µL chitosan nanoparticles were added to the medium for 6 hours. The ADSCs were examined by

flow cytometry 48 hours after transfection to evaluate the transfection efficiency.

Physicochemical characterization of chitosan nanoparticles

Chitosan-plasmid nanoparticles were subjected to 0.8% agarose gel electrophoresis followed by ethidium bromide staining and ultraviolet imaging. For morphological observation, the chitosan-plasmid nanoparticles were diluted 1:15 with 30 mmol/L Na₂SO₄, fixed on clean mica, and dried with N₂. The nanoparticles were then examined using an atomic force microscope (SPI3800N, DI instrument Nanoscope 3D Multimode SPM; Veeco, CA, USA) and dynamic light scattering (Malvern Instruments, Malvern, UK).

Real-time polymerase chain reaction (PCR)

Total RNA was isolated from ADSCs and reverse transcribed to cDNA using cDNA Synthesis Kits (Takara, Tokyo, Japan) according to the manufacturer's instructions. PCR primers were designed using Primer 5 software. The PCR primers (Nanjing Sirui Technology Co. Ltd.) used are listed in Table 1. Real-time PCR reactions were carried out using the MultiGene Gradient System (Labnet, NJ, USA) in a 96-well clear optical reaction plate with optical adhesive covers. Reactions were run in duplicate in 5 µL, including 2 µL of cDNA solution and 3 µL of a homemade target-specific mix composed of 5/6 2×Power SYBR Green Master Mix (Toyobo, Japan) and 1/6 100 mM primer solution. The PCR program was: 95°C for 10 minutes, followed by 40 cycles of 15 s at 95°C, and 1 minute at 60°C. PCR was carried out using a 7500 Fast Real-Time PCR system, and the data were analyzed with 7500 software v2.0.1 (both Applied Biosystems, Foster City, CA, USA).

Table 1. Primer design for real-time polymerase chain reaction.

Gene	Forward primer	Reverse primer
BMP-2	CCAAGATGAACACAGCTGGTCACAGA	CCCACGTCACTGAAGTCCACG
FGF2	GGAGAAGAGCGACCCTCACATCA	GCCAGGTAACGGTTAGCACACACT
18S rRNA	GACTCAACACGGGAAACCTCAC	CCAGACAAATCGCTCCACCAAC
BSP	CGAACAAAGGCATAAACGGCACCA	CTCCATTGTCTTCTCCGCTGCT
OCN	CAGTTCTGCTCCTCTCCAGGCA	CATCCATAGGGCTGGGAGGTCA

BMP-2, bone morphogenetic protein-2; FGF2, fibroblast growth factor 2; BSP, bone sialoprotein; OCN, osteocalcin.

Enzyme-linked immunosorbent assay (ELISA)

The concentrations of human BMP-2 and FGF2 proteins in the supernatants of the cultured ADSCs were detected by ELISA (Invitrogen, MA, USA) according to the manufacturer's instructions.

Western blot analysis

ADSCs were collected in RIPA buffer (containing 0.2% Triton X-100, 5 mmol/L EDTA, 1 mmol/L phenylmethylsulfonyl fluoride, 10 µg/mL leupeptin, 10 µg/mL aprotinin, and 100 mmol/L NaF and 2 mmol/L Na₃VO₄) and lysed for 30 minutes on ice. Protein concentrations were assayed using a Bio-Rad protein kit (Hercules, CA, USA). Equal amounts of sample per well were loaded in a sodium dodecyl sulfate-polyacrylamide gel. The proteins were then transferred onto 0.45-µm pore-size positively-charged polyvinylidene difluoride membranes (Millipore, Germany) and blocked with 5% dry milk in PBS with 0.1% Tween-20 at room temperature. The blots were challenged with primary antibodies in blocking solution overnight at 4°C, washed three times with PBST (0.1% Tween-20), and challenged with horseradish peroxidase-conjugated goat anti-rabbit, rabbit anti-goat, or mouse anti-mouse antibodies, respectively, followed by detection with an enhanced chemiluminescent substrate (Pierce, Rockford, IL, USA). The primary antibodies were mouse monoclonal anti-

BMP-2 (Abcam, Cambridge, MA, USA), rabbit polyclonal anti-FGF2 (Abcam), or mouse monoclonal anti-β-Actin (Santa Cruz Biotechnology, Santa Cruz, CA, USA).

Cell Counting Kit-8 (CCK-8) and lactate dehydrogenase (LDH) release assays

ADSCs were disseminated in 96-well plates at a concentration of 2000 cells per well and then transfected with *BMP2* and/or *FGF2*. After 24 hours, the viability of the ADSCs and cytotoxic effects were determined using a CCK-8 kit (Dojindo, Japan) and a LDH release kit (Beyotime Institute of Biotechnology, Jiangsu, China), respectively, according to the manufacturer's instructions.^{15,16}

Statistical analysis

Data were analyzed using SPSS Statistics for Windows, Version 19.0 (SPSS Inc., Armonk, NY: IBM Corp, USA). Data were expressed as mean ± standard error of the mean. One-way ANOVA or two-way repeated measures ANOVA was used for multiple group comparisons. A probability of $P < 0.05$ was considered statistically significant.

Results

Physicochemical characterization of chitosan nanoparticles

We characterized the physicochemical properties of the chitosan nanoparticles

using nano-atomic force microscopy. The Solarbio chitosan nanoparticles were larger and showed more precipitation than the Sigma nanoparticles (Figure 2a-d). We therefore used the Sigma chitosan nanoparticles for all subsequent experiments. The chitosan–plasmid nanoparticles were irregularly spherical with a compact structure. The particle size was uniformly about 200 nm and the zeta potential was 30 mV, suggesting that the chitosan nanoparticles had been prepared successfully (Figure 2e and 2f).

Human ADSC culture, identification, and transfection

ADSCs were examined morphologically under an inverted microscope. After a further

7 days of culture, the ADSCs became spindle shaped and merged to form adherent cell clusters (Figure 3a). FACS analysis showed expression of the ADSC markers CD44, CD29, and CD105 in the cultured ADSCs (99.5%, 99.3%, and 86.8%, respectively) (Figure 3b-d), but only a few cells (1.42%) expressed the immune cell marker CD45 (Figure 3e). These results suggested successful culture of human ADSCs *in vitro*.

We also assessed the transfection efficiency by FACS analysis. After 48 hours of co-transfection, $19.03\% \pm 1.74\%$ of cells expressed BMP2-EGFP and FGF2-RFP, $14.13\% \pm 3.06\%$ only expressed FGF2-RFP, $22.53 \pm 3.94\%$ only expressed BMP-EGFP, and $44.30\% \pm 5.21\%$ of cells expressed neither. These results indicated

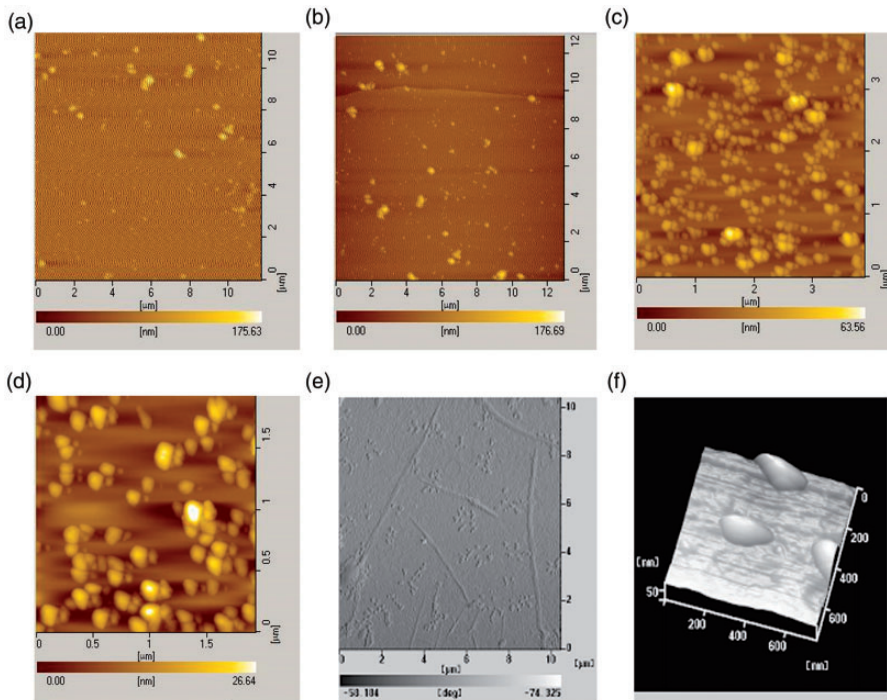


Figure 2. Physicochemical characterization of chitosan nanoparticles by nano-atomic force microscopy. (a, b) The Solarbio chitosan nanoparticles were larger and showed more precipitation; (c, d) the Sigma chitosan nanoparticles were smaller, with no precipitation. At higher definition, the chitosan–plasmid nanoparticles were generally spherical, but could also be irregular, with compact structure. The particle size was about 200 nm (e, f).

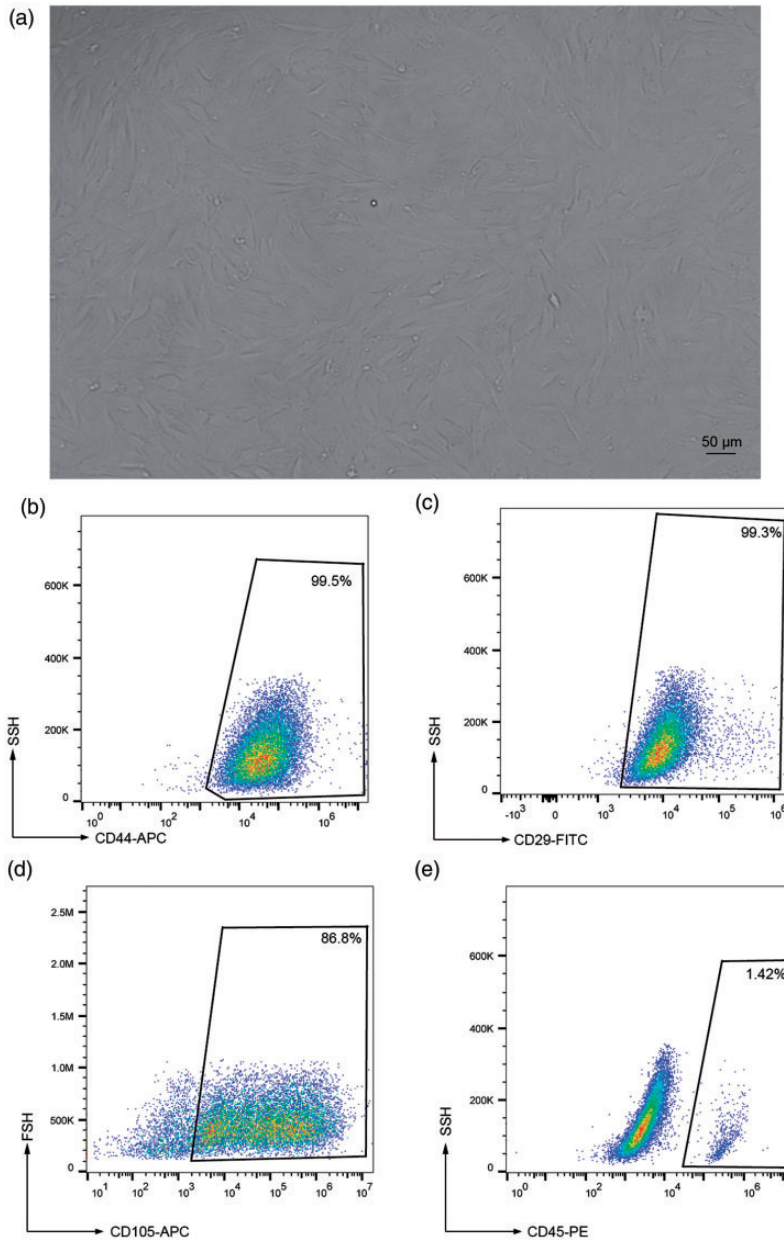


Figure 3. Characterization of human adipose-derived stromal cells (ADSCs) *in vitro*. (a) ADSCs became spindle shaped and formed adherent clusters after 7 days in culture. (b-e) Fluorescence-activated cell sorting showed expression of CD44, CD29, CD105, and CD45 in cultured ADSCs, confirming their stem cell nature. Values expressed as mean \pm standard error (n=4). APC, allophycocyanin; FITC, fluorescein isothiocyanate; PE, phycoerythrin.

that both pEGFP-N2-hBMP-2 and pTagRFP-C-hFGF2 were successfully transfected (Figure 4a and 4b).

FGF2 and BMP2 mRNA levels after transfection

To explore if the transfected ADSCs expressed BMP2 and/or FGF2, we detected

the respective mRNA levels of these genes by real-time PCR. *FGF2* and *BMP2* mRNA levels were up-regulated in the co-transfection group compared with the control group (7.87-fold change, $P < 0.001$; 3.1-fold change, $P < 0.001$, respectively). However, the *FGF2* and *BMP2* mRNA levels were slightly lower

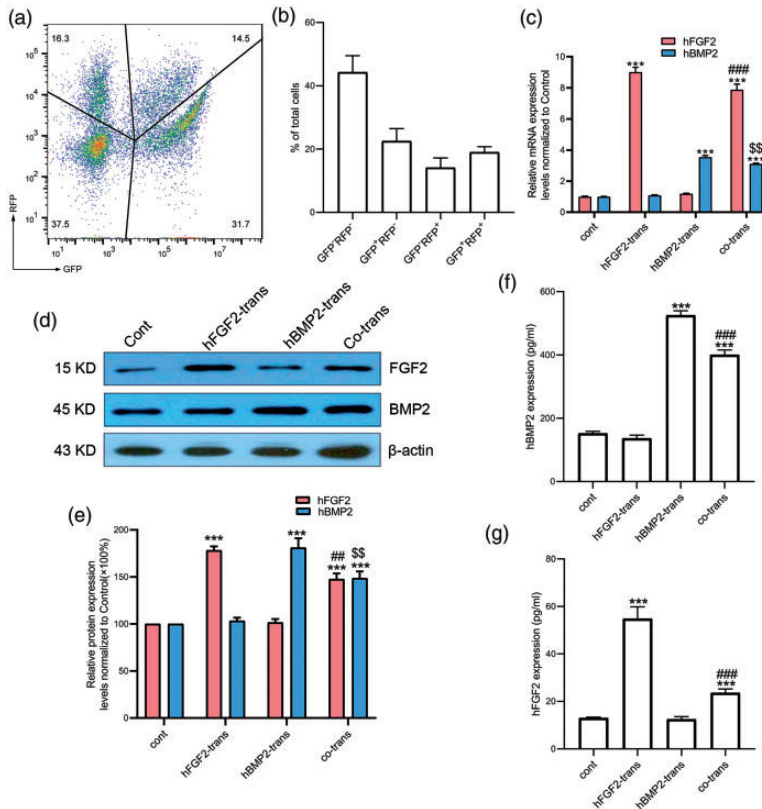


Figure 4. Successful transfection of human adipose-derived stromal cells (ADSCs) with BMP2 and FGF2. (a, b) At 48 hours after transfection, pTagRFP-C-hFGF2 plasmid caused expression of red fluorescent protein (RFP) and pEGFP-N2-Hu-BMP2 plasmid caused expression of green fluorescent protein (GFP) in ADSCs. (c) Relative mRNA expression levels of *FGF2* and *BMP2* ($n=6$ from 3 independent experiments). $***P < 0.001$ vs control group, $####P < 0.001$ vs *FGF2*-transfected group, $$$P < 0.01$ vs *BMP2*-transfected group. (d, e) Western blotting showed the protein expression levels of FGF2 and BMP-2 ($n=4$ from 2 independent experiments). $***P < 0.001$ vs control group, $##P < 0.01$ vs *FGF2*-transfected group, $$$P < 0.01$ vs *BMP2*-transfected group. (f) Protein expression pattern of BMP-2 levels in cell supernatants ($n=3$ from 3 independent experiments) determined by enzyme-linked immunosorbent assay (ELISA). $***P < 0.001$ vs control group, $####P < 0.001$ vs *BMP2*-transfected group. (g) Protein expression pattern of the FGF2 in cell supernatants ($n=3$ from 3 independent experiments) determined by ELISA. $***P < 0.001$ vs control group, $####P < 0.001$ vs *FGF2*-transfected group. Values given as mean \pm standard error. trans, transfected; cont, control; h, human.

than in the corresponding single-gene transfection groups (7.87 ± 0.15 vs 9.00 ± 0.13 , $P < 0.001$; 3.11 ± 0.02 vs 3.54 ± 0.02 , $P < 0.01$, respectively) (Figure 4c). These results indicated that transfection with the vectors containing *FGF2* and *BMP2* led to transcription of the respective genes in the ADSCs.

FGF2 and BMP-2 protein levels after transfection

FGF2 and BMP-2 protein expression levels were increased 1.47-fold and 1.49-fold in the co-transfection group compared with the control group (Figure 4d and 4e). However, the protein expression levels in the co-transfection group were significantly lower than in the corresponding single-gene transfection groups ($147.67\% \pm 6\%$ vs $178.3\% \pm 4.1\%$, $P < 0.01$; $148.7\% \pm 7.2\%$ vs $181.22\% \pm 9.9\%$, $P < 0.01$, respectively). These results suggest that chitosan-mediated co-transfection of *BMP2/FGF2* into human ADSCs resulted in expression of the respective proteins.

Secretion of FGF2 and BMP-2 in cell supernatant

We evaluated the release of FGF2 and BMP-2 into the cell supernatant by ELISA. Both FGF2 and BMP-2 protein expression levels were up-regulated in the co-transfection group compared with the control group, consistent with the results of western blotting. There was no significant difference in FGF2 levels between the *BMP2*-transfected and control groups, and no significant difference in BMP-2 levels between the *FGF2*-transfected and control groups (Figure 4f and 4g). This indicated that vector-induced expression of one factor did not influence the expression of the other factor in terms of local release, suggesting the importance of co-expression of *BMP2* and *FGF2*.

Viability and osteogenic ability of ADSCs and assessment of cytotoxic effects after transfection with BMP2 and/or FGF2

We explored the cell viability and cytotoxic effects of transfection on ADSCs by CCK-8 and LDH release assays, respectively. The viability of ADSCs increased significantly after transfection with *BMP2* or *FGF2*, with the greatest effect following co-transfection with both genes (Figure 5a). In addition, there were no obvious toxic effects in ADSCs transfected with *BMP2* and/or *FGF2* (Figure 5b).

We evaluated the mRNA expression levels of OCN and BSP to explore the effects of gene co-transfection via chitosan nanoparticles on osteogenesis in ADSCs. OCN and BSP mRNA levels were significantly higher in the co-transfection group compared with the single-gene transfection groups and the control group, suggesting significant enhancement of osteogenesis (Figure 5c and 5d).

Discussion

Gene therapy for bone defects involves the local transfection of target cells with osteogenic genes that can be transcribed and translated into proteins. Expression of the proteins stimulates the target cells, thereby promoting bone formation via autocrine or paracrine mechanisms. Gene therapy ensures the targeted release of the gene product, maximizes the local therapeutic effect, and reduces systemic side effects. Moreover, several genes can be transduced together, leading to synergistic regulation of endogenous protein synthesis, and enhanced biological activity compared with the administration of exogenous recombinant proteins. Gene therapy is thus considered as the most promising therapy for maintaining an effective local therapeutic concentration of growth factors to aid the repair of partial bone defects.¹⁷⁻¹⁹

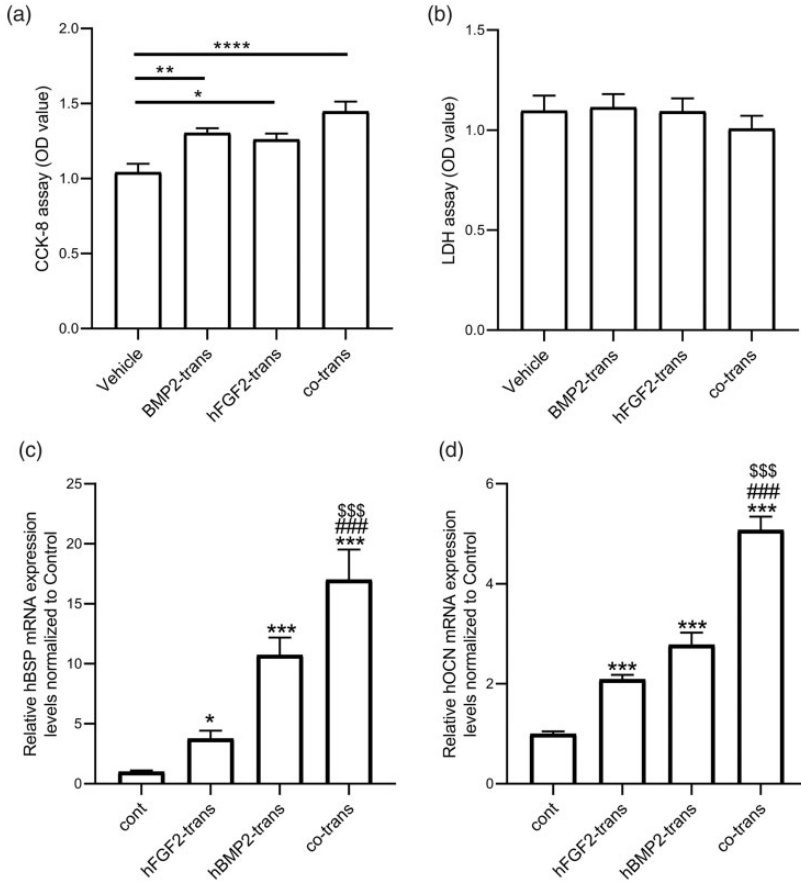


Figure 5. Co-transfection of *BMP2* and *FGF2* via chitosan nanoparticles increased cell viability and osteogenic ability of human adipose-derived stromal cells (ADSCs) *in vitro*. The cell viability and cytotoxic effects on ADSCs were measured by (a) Cell Counting Kit-8 (CCK-8) and (b) lactate dehydrogenase (LDH) assays, respectively ($n = 6$ from 3 independent experiments). $*P < 0.05$, $**P < 0.01$, $***P < 0.0001$. Relative mRNA expression levels of (c) osteocalcin (OCN) and (d) bone sialoprotein (BSP) (d) showed that co-transfection had a synergistic effect on osteogenesis, evidenced by higher expression of the osteogenesis markers BSP and OCN compared with single-gene transfection. Values given as mean \pm standard error ($n = 6$ from 3 independent experiments). $***P < 0.001$ vs control group, $####P < 0.001$ vs *FGF2*-transfected group, $$$$P < 0.001$ vs *BMP2*-transfected group. OD, optical density; trans, transfected; cont, control.

ADSCs isolated from the blood vessels of adipose tissue exhibit similar morphology, immunophenotype, and differentiation properties to mesenchymal stem cells from bone marrow (BMSCs) and umbilical cord blood. Numerous studies have shown that ADSCs have the potential to differentiate into fat, bone, cartilage, and muscle derived

from mesoderm.^{20–22} Single-cell cloning experiments have confirmed the pluripotent differentiation of ADSCs.^{23,24} Although BMSCs were the first to be found to have osteogenic potential and were thus considered as seed cells for bone tissue engineering,^{25,26} the number of BMSCs in the bone marrow is limited, and although *in vitro*

expansion can produce large numbers of cells, it also leads to the loss of stem cell characteristics and potential changes in the differentiation potential.^{27,28} Compared with BMSCs, ADSCs have several advantages, such as a wide variety of sources, rich content, little trauma to the donor during harvesting, and *in vitro* amplification capability.^{24,29} ADSCs have thus become an important source of seed cells for bone tissue engineering.

BMP-2 plays an important role in bone formation and healing.³⁰⁻³³ Moreover, Bouyer et al.³⁴ and Tarek et al.³⁵ developed effective delivery systems using film-coated poly(lactic-co-glycolic acid) (PLGA) and PLGA/magnesium hydroxide scaffolds to improve the *in vivo* bone regeneration potential of BMP-2. Recombinant human BMP-2 is the only drug approved by the U.S. Food and Drug Administration as an osteogenesis-promoting factor.³² Dragoo et al.³⁶ first reported the deposition of large amounts of calcium in the extracellular matrix *in vitro* after virally mediated *BMP2* gene transfection in human ADSCs. *In vivo* studies showed the formation of bone marrow cavity cells after transfection with *BMP2*, compared with fat-like tissue in the control group.³⁷ OCT4 has been suggested to act as a downstream mediator for BMP-induced bone regeneration.³⁸ Panetta et al.³⁹ demonstrated that exogenous human ADSC recombinant human BMP-2 could significantly enhance osteoblast activity *in vitro* in a concentration-dependent manner. Down-regulation of the nuclear factor- κ B signaling pathway was suggested to be involved in BMP-2-mediated repair of articular cartilage via upregulation of angiogenesis factors.⁴⁰ Other BMP family proteins, including BMP-9, can also promote osteoblastic differentiation of MSCs both *in vitro* and *in vivo*, but probably via different mechanisms.⁴¹ FGF2 is a polypeptide that promotes cell growth and bone tissue

repair, and exogenous FGF2 was shown to promote bone formation;⁴² however, exogenous FGF2 is easily degraded within the body, thus reducing its efficacy.⁴³ The *FGF2* gene can now be transfected into osteoblasts, leading to over-expression of FGF2 protein and the promotion of osteogenesis *in vivo*. FGF-2 and BMP-2 have demonstrated synergistic effects on bone induction *in vivo* via the extracellular signal-regulated kinase signaling pathway.⁴⁴ Peroxisome proliferator-activated receptor- γ and Runt-related transcription factor 2 have been suggested to be the two major transcription factors involved at various intersecting signaling pathways regulating adipogenesis and osteogenesis.⁴⁵ Interestingly, in addition to commonly recognized cell components such as osteoblasts and osteoclasts, emerging evidence also supports the role of macrophages as immunomodulators for the various cytokines involved during the bone regeneration process.⁴⁶

Biomaterial scaffolds have been used extensively to deliver growth factors to induce new bone formation.^{47,48} Chitosan, as a non-viral gene vector, is both biocompatible and biodegradable, and is also a safe and easy-to-construct polymer molecule that can protect DNA from degradation.⁴⁹ Most previous studies have been based on the expression of individual genes via viral vectors, while the main innovation of the current study involved the use of chitosan nanoparticles as a non-viral gene transfer vector for multiple genes, to produce a synergistic effect on osteoblasts. We successfully constructed high-performance chitosan nanoparticles carrying *BMP2* and *FGF2* genes, which could co-transfect both these genes into human ADSCs, resulting in BMP-2/FGF2 protein expression. Importantly, our results showed good synergy between the two plasmids, resulting in a significantly higher osteogenic index

(i.e. BSP and OCN) compared with transfection with either gene alone.

This study had several limitations. First, we were not able to analyze the direct uptake of nanoparticles into the cells owing to our laboratory capacity. However, co-transfection of *BMP2* and *FGF2* via chitosan nanoparticles showed good efficiency, indirectly indicating the successful entry of the nanoparticles into the cells. Second, we could not assess the *in vivo* osteogenic efficacy of the chitosan nanoparticles co-transfected with *BMP2* and *FGF2* owing to the lack of a suitable animal model. However, further experiments are planned to address this in the future.

Conclusion

The results of this preliminary study suggest that co-transfection of *BMP2* and *FGF2* by chitosan nanoparticles into human ADSCs has a good synergistic osteogenic effect.


Declaration of conflicting interest

The authors declare that there is no conflict of interest.

Funding

The author(s) disclosed receipt of the following financial support for the research, authorship, and/or publication of this article: This work was supported by the Zhejiang Provincial Medical and Healthy Science Foundation of China [grant number 2019ZD028], the National Key Research Program of China [grant number 2016YFC1101004], and the National Natural Science Foundation of China [grant number 81671918].

ORCID iDs

Ying Hu  <https://orcid.org/0000-0003-4558-9878>

Wei-Qiang Tan  <https://orcid.org/0000-0003-4951-0960>

References

1. Obremeskey WT, Molina CS, Collinge C, et al. Current practice in the management of segmental bone defects among orthopaedic trauma surgeons. *J Orthop Trauma* 2013.
2. Nair MB, Kretlow JD, Mikos AG, et al. Infection and tissue engineering in segmental bone defects—a mini review. *Curr Opin Biotechnol* 2011; 22: 721–725.
3. Delhove J, Osenk I, Prichard I, et al. Public acceptability of gene therapy and gene editing for human use: a systematic review. *Hum Gene Ther* 2020; 31: 20–46.
4. Hitti FL, Gonzalez-Alegre P and Lucas TH. Gene therapy for neurologic disease: a neurosurgical review. *World Neurosurg* 2019; 121: 261–273.
5. Liu Y, Yang S, Cao L, et al. Facilitated vascularization and enhanced bone regeneration by manipulation hierarchical pore structure of scaffolds. *Mater Sci Eng C Mater Biol Appl* 2020, 110: 110622.
6. Zhang M, Matinlinna JP, Tsoi JKH, et al. Recent developments in biomaterials for long-bone segmental defect reconstruction: A narrative overview. *J Orthop Translat* 2020; 22: 26–33.
7. Buchtova M, Oralova V, Aklian A, et al. Fibroblast growth factor and canonical WNT/beta-catenin signaling cooperate in suppression of chondrocyte differentiation in experimental models of FGFR signaling in cartilage. *Biochim Biophys Acta* 2015; 1852: 839–850.
8. Jiang N, He J, Zhang W, et al. Directed differentiation of BMSCs on structural/compositional gradient nanofibrous scaffolds for ligament-bone osteointegration. *Mater Sci Eng C Mater Biol Appl* 2020; 110: 110711.
9. Franceschi RT, Yang S, Rutherford RB, et al. Gene therapy approaches for bone regeneration. *Cells Tissues Organs* 2004; 176: 95–108.
10. Gromolak S, Krawczenko A, Antończyk A, et al. Biological characteristics and osteogenic differentiation of ovine bone marrow derived mesenchymal stem cells stimulated with FGF-2 and BMP-2. *Int J Mol Sci* 2020; 21: 9726.

11. Huang T, Song X, Jing J, et al. Chitosan-DNA nanoparticles enhanced the immunogenicity of multivalent DNA vaccination on mice against *Trueperella pyogenes* infection. *J Nanobiotechnology* 2018; 16: 8.
12. Baghdan E, Pinnapireddy SR, Strehlow B, et al. Lipid coated chitosan-DNA nanoparticles for enhanced gene delivery. *Int J Pharm* 2018; 535: 473–479.
13. Peng W, Gao T, Yang ZL, et al. Adipose-derived stem cells induced dendritic cells undergo tolerance and inhibit Th1 polarization. *Cell Immunol* 2012; 278: 152–157.
14. Omwoyo WN, Ogutu B, Oloo F, et al. Preparation, characterization, and optimization of primaquine-loaded solid lipid nanoparticles. *Int J Nanomedicine* 2014; 9: 3865–3874.
15. Wang J, Li H, Ren Y, et al. Local delivery of β -elemene improves locomotor functional recovery by alleviating endoplasmic reticulum stress and reducing neuronal apoptosis in rats with spinal cord injury. *Cell Physiol Biochem* 2018; 49: 595–609.
16. Wang J, Li H, Yao Y, et al. β -Elemene enhances GAP-43 expression and neurite outgrowth by inhibiting RhoA kinase activation in rats with spinal cord injury. *Neuroscience* 2018; 383: 12–21.
17. Bez M, Pelled G and Gazit D. BMP gene delivery for skeletal tissue regeneration. *Bone* 2020; 137: 115449.
18. Dohrn MF, Auer-Grumbach M, Baron R, et al. Chance or challenge, spoilt for choice? New recommendations on diagnostic and therapeutic considerations in hereditary transthyretin amyloidosis with polyneuropathy: the German/Austrian position and review of the literature. *J Neurol* 2020. doi: 10.1007/s00415-020-09962-6.
19. Ilaltdinov AW, Gong Y, Leong DJ, et al. Advances in the development of gene therapy, noncoding RNA, and exosome-based treatments for tendinopathy. *Ann N Y Acad Sci* 2020. doi: 10.1111/nyas.14382.
20. Kunze KN, Burnett RA, Wright-Chisem J, et al. Adipose-derived mesenchymal stem cell treatments and available formulations. *Curr Rev Musculoskelet Med* 2020; 13: 264–280.
21. Mazini L, Rochette L, Admou B, et al. Hopes and limits of adipose-derived stem cells (ADSCs) and mesenchymal stem cells (MSCs) in wound healing. *Int J Mol Sci* 2020; 21: 1306.
22. Shukla L, Yuan Y, Shayan R, et al. Fat therapeutics: the clinical capacity of adipose-derived stem cells and exosomes for human disease and tissue regeneration. *Front Pharmacol* 2020; 11: 158.
23. Mazini L, Rochette L, Amine M, et al. Regenerative capacity of adipose derived stem cells (ADSCs), comparison with mesenchymal stem cells (MSCs). *Int J Mol Sci* 2019; 20: 2523.
24. Zhou W, Lin J, Zhao K, et al. Single-cell profiles and clinically useful properties of human mesenchymal stem cells of adipose and bone marrow origin. *Am J Sports Med* 2019; 47: 1722–1733.
25. Li C, Wei G, Gu Q, et al. Donor age and cell passage affect osteogenic ability of rat bone marrow mesenchymal stem cells. *Cell Biochem Biophys* 2015; 72: 543–549.
26. El Refaey M, Watkins CP, Kennedy E, et al. Oxidation of the aromatic amino acids tryptophan and tyrosine disrupts their anabolic effects on bone marrow mesenchymal stem cells. *Mol Cell Endocrinol* 2015; 410: 87–96.
27. Palombella S, Lopa S, Gianola S, et al. Bone marrow-derived cell therapies to heal long-bone nonunions: a systematic review and meta-analysis-which is the best available treatment? *Stem Cells Int* 2019; 2019: 3715964.
28. Zhang R, Ma J, Han J, et al. Mesenchymal stem cell related therapies for cartilage lesions and osteoarthritis. *Am J Transl Res* 2019; 11: 6275–6289.
29. Delanois RE, Etcheson JI, Sodhi N, et al. Biologic therapies for the treatment of knee osteoarthritis. *J Arthroplasty* 2019; 34: 801–813.
30. Shakir S, MacIsaac ZM, Naran S, et al. Transforming growth factor beta 1 augments calvarial defect healing and promotes suture regeneration. *Tissue Eng Part A* 2015; 21: 939–947.
31. Carpenter RS, Goodrich LR, Frisbie DD, et al. Osteoblastic differentiation of human

- and equine adult bone marrow-derived mesenchymal stem cells when BMP-2 or BMP-7 homodimer genetic modification is compared to BMP-2/7 heterodimer genetic modification in the presence and absence of dexamethasone. *J Orthop Res* 2010; 28: 1330–1337.
32. Parsa A, Vahedi H, Goswami K, et al. Available findings fail to provide strong evidence of the role of bone morphogenic protein-2 in femoral head osteonecrosis. *Arch Bone Jt Surg* 2020; 8: 5–10.
 33. Mariscal G, Nunez JH, Barrios C, et al. A meta-analysis of bone morphogenic protein-2 versus iliac crest bone graft for the posterolateral fusion of the lumbar spine. *J Bone Miner Metab* 2020; 38: 54–62.
 34. Bouyer M, Guillot R, Lavaud J, et al. Surface delivery of tunable doses of BMP-2 from an adaptable polymeric scaffold induces volumetric bone regeneration. *Biomaterials* 2016; 104: 168–181.
 35. Bedair TM, Lee CK, Kim DS, et al. Magnesium hydroxide-incorporated PLGA composite attenuates inflammation and promotes BMP2-induced bone formation in spinal fusion. *J Tissue Eng* 2020; 11: 2041731420967591.
 36. Dragoo JL, Lieberman JR, Lee RS, et al. Tissue-engineered bone from BMP-2-transduced stem cells derived from human fat. *Plast Reconstr Surg* 2005; 115: 1665–1673.
 37. Xu G, Yamamoto N, Nojima T, et al. The process of bone regeneration from devitalization to revitalization after pedicle freezing with immunohistochemical and histological examination in rabbits. *Cryobiology* 2020; 92: 130–137.
 38. Kim SHL, Lee SS, Kim I, et al. Ectopic transient overexpression of OCT-4 facilitates BMP4-induced osteogenic transdifferentiation of human umbilical vein endothelial cells. *J Tissue Eng* 2020; 11: 2041731420909208.
 39. Panetta NJ, Gupta DM, Lee JK, et al. Human adipose-derived stromal cells respond to and elaborate bone morphogenetic protein-2 during in vitro osteogenic differentiation. *Plast Reconstr Surg* 2010; 125: 483–493.
 40. Wang C, Zang H and Zhou D. Bone morphogenetic protein-2 exhibits therapeutic benefits for osteonecrosis of the femoral head through induction of cartilage and bone cells. *Exp Ther Med* 2018; 15: 4298–4308.
 41. Beederman M, Lamplot JD, Nan G, et al. BMP signaling in mesenchymal stem cell differentiation and bone formation. *J Biomed Sci Eng* 2013; 6: 32–52.
 42. Hsieh MJ, Huang C, Lin CC, et al. Basic fibroblast growth factor promotes doxorubicin resistance in chondrosarcoma cells by affecting XRCC5 expression. *Mol Carcinog* 2020; 59: 293–303.
 43. Guo Y, Xu B, Wang Y, et al. Dramatic promotion of wound healing using a recombinant human-like collagen and bFGF cross-linked hydrogel by transglutaminase. *J Biomater Sci Polym Ed* 2019; 30: 1591–1603.
 44. Song R, Wang D, Zeng R, et al. Synergistic effects of fibroblast growth factor-2 and bone morphogenetic protein-2 on bone induction. *Mol Med Rep* 2017; 16: 4483–4492.
 45. James AW. Review of signaling pathways governing MSC osteogenic and adipogenic differentiation. *Scientifica (Cairo)* 2013; 2013: 684736.
 46. Niu Y, Wang Z, Shi Y, et al. Modulating macrophage activities to promote endogenous bone regeneration: Biological mechanisms and engineering approaches. *Bioact Mater* 2021; 6: 244–261.
 47. King WJ and Krebsbach PH. Growth factor delivery: how surface interactions modulate release in vitro and in vivo. *Adv Drug Deliv Rev* 2012; 64: 1239–1256.
 48. De Witte TM, Fratila-Apachitei LE, Zadpoor AA, et al. Bone tissue engineering via growth factor delivery: from scaffolds to complex matrices. *Regen Biomater* 2018; 5: 197–211.
 49. Veilleux D, Nelea M, Biniecki K, et al. Preparation of concentrated chitosan/DNA nanoparticle formulations by lyophilization for gene delivery at clinically relevant dosages. *J Pharm Sci* 2016; 105: 88–96.